HHS Public Access

Author manuscript

J Control Release. Author manuscript; available in PMC 2018 February 10.

Published in final edited form as:

J Control Release. 2017 February 10; 247: 167–174. doi:10.1016/j.jconrel.2017.01.006.

Longitudinal monitoring of skin accumulation of nanocarriers and biologicals with fiber optic near infrared fluorescence spectroscopy (FONIRS)

James I. Griffin[1], **Michael J. Benchimol**[2], and **Dmitri Simberg**[1]

[1]The Skaggs School of Pharmacy and Pharmaceutical Sciences, University of Colorado Anschutz Medical Campus, 12850 East Montview Blvd., Aurora, CO 80045, USA

[2]Sonrgy Inc., 10655 Sorrento Valley Rd., San Diego, CA 92121

Abstract

Systemically injected drug delivery systems distribute into various organs and tissues, including liver, spleen and kidneys. Recent reports pointed out a significant accumulation of systemically injected nanoparticles in the skin. Skin constitutes the largest organ in the body with important immune functions, and accumulation of drug delivery systems could have significant implications for skin toxicity in living subjects. Fiber optic-based near-infrared spectroscopy (FONIRS) setup was developed and tested for measuring of NIR (760nm excitation) emission spectra in the skin. Ex vivo spectral measurements of NIR fluorescence through the skin showed linear response down to 34 femtomole of dye DiR. Following systemic injection of IRDye 800 labeled 500kDa dextran, FONIRS detected an immediate and stable accumulation of fluorescence in the skin. Longitudinal monitoring of skin accumulation and elimination of IRDye 800-labeled therapeutic anti-epidermal growth factor antibody (cetuximab) showed significant signal in the skin after the antibody cleared from circulation. Comparison of skin accumulation of DiR labeled, long-circulating PEGylated liposomes with short-circulating non-PEGylated liposomes showed much higher accumulation of PEGylated liposomes that persisted several days after the liposomes cleared from blood. Measurements with FONIRS enabled to estimate skin concentration of liposomes (percent of injected dose per gram). This simple and practical approach can be used to monitor accumulation of drug delivery systems in preclinical and clinical studies.

Graphical abstract

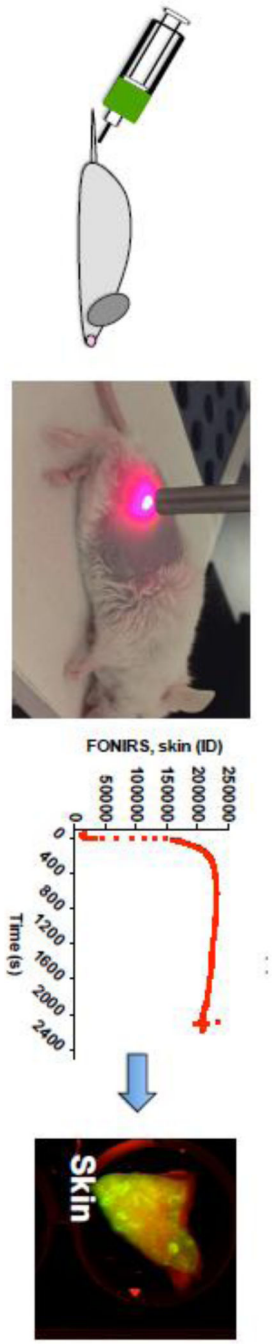

INTRODUCTION

Modern pharmaceutical science has been witnessing an exciting renaissance in drug delivery technologies. In particular, engineered nanoparticles, polymers, and biologicals have a promise to greatly improve safety and efficacy of treatment of diseases. At the same time, these compounds have not demonstrated precise selectivity for diseased tissues alone; e.g., tumors, and often distribute throughout the body into healthy tissues and organs [1]. In

addition to the main clearance organs (liver, spleen, and kidneys), deposition in other tissues could have a significant impact on safety and toxicity in human patients [2]. For instance, one of the most frequent and peculiar dose limiting toxicities of liposomal doxorubicin is skin toxicity, manifested by severe pain and ulceration in palms, feet, and in areas of pressure (palmar-plantar erythrodysesthesia, *aka* hands and feet syndrome)[3, 4]. This phenomenon is likely caused by accumulation of long-circulating liposomes in the dermis and deposition of an anticancer drug [4]. Accumulation in the skin is not limited to liposomes, and recent evidence suggests that gold nanoparticles, silica and quantum dots distribute into the skin following systemic injection [5, 6]. Biologicals are also known to accumulate in the skin as exemplified by severe dose-limiting skin toxicity of anti-EGFR antibody cetuximab (Erbitux™) used to treat lung and colorectal cancers [7].

In the light of the above evidence, there is an immense need for non-invasive tools to monitor deposition of xenobiotic drug delivery systems in humans. Of all organs that accumulate nanocarriers, skin is of high interest because it is the largest organ in the body (~16% body weight) and it performs multiple functions including immunity. Skin is easy to monitor and access, and skin color has been historically used to assess accumulation of drugs in the body, for example, blue color (chrysiasis) due to colloidal gold in arthritis, discoloration due to chloroquine, and skin pigmentation due to tetracycline antibiotics [8]. Albeit skin biopsies can be used to measure skin exposure, they are not convenient and cannot sample the entire body. Most nanoparticles except quantum dots and gold [9, 10] produce very little if any intrinsic fluorescence or Raman spectra of sufficient intensity to enable measurements in the skin. However, drug delivery systems can be easily tagged with fluorescent or Raman tags [10]. Raman spectroscopy has certain limitations due to low sensitivity and usually only works well for photonic materials [11]. On the other hand, fluorescence is arguably one of the cheapest and attractive imaging modalities that allows penetrating several millimeters of tissue in the near-infrared (NIR) window [12]. Several commercially-available NIR fluorophores with high quantum yield have been clinically approved or are at different stages of clinical testing (i.e., IRDye 700 conjugated anti-EGFR antibody (clinical trial identifier NCT02422979) and indocyanine for fluorescence guided surgery)[13, 14], making fluorescent tagging of drug delivery systems an attractive, clinically viable option.

Several *in vivo* fluorophore detection systems based on NIR fluorescence spectroscopy, digital imaging, and luminescence have been described [15]. Compared to imaging, spectroscopy is a very attractive modality because of its speed, low cost, and sensitivity [15, 16], but its utility for skin monitoring has not been investigated before. Here, we designed a portable fiber optic-based NIR spectrometry setup (FONIRS) and demonstrated feasibility of longitudinal monitoring of skin accumulation of fluorescently tagged drug delivery systems.

MATERIALS AND METHODS

Materials

IRDye 680RD NHS Ester (IRDye 680) and IRDye 800CW NHS Ester (IRDye 800) were ordered from Li-COR (Lincoln, NE, USA). Amino-dextrans 500kDa and 3kDa were from Thermo Fisher. Egg phosphatidylcholine and DSPE-PEG 2000 were from Avanti Polar

Lipids (Alabaster, AL, USA), DiR (1,1'-Dioctadecyl-3,3,3',3'-Tetramethylindotricarbocyanine Iodide) was from Biotium (Hayward, CA, USA). Whatman Nucleopore Track-Etch Membranes (0.2μm pore size) were from Sigma-Aldrich (St. Louis, MO, USA). Cetuximab (ERBITUX™) was obtained from the University of Colorado Cancer Center pharmacy. Nitrocellulose membrane was from Bio-Rad. Collagenase type IV was from Sigma.

FONIRS

The system consisted of a Maya 2000 Pro spectrometer with OceanView 1.5.0 software (both Ocean Optics) connected to a custom-built 600μm-excitation/emission probe via fiber-optic bundle (all from Ocean Optics, San Jose, CA). The system can perform extremely fast measurements of entire spectra with a handheld probe and has the ability to analyze and integrate spectra over a desired range for comparative spectroscopy. The FONIRS system used LED with a peak emission wavelength of 760nm as an excitation light source (Prizmatix Ltd., Givat-Shmuel, Israel). The in-line BrightLine® filters (Semrock Inc., Rochester NY) were 785nm short-pass (excitation) and 785nm long-pass (emission) for 760nm LED. The emission was collected over a range of 800–840nm. The reported integrated fluorescence (IF) values are an integration of the spectral intensity over the appropriate range.

In vitro and *ex vivo* sensitivity with FONIRS and Li-COR

DiR dye was dissolved in DMSO, and the concentration was quantified with a Thermo Scientific BioMate 3S Spectrophotometer. The dye was then serially diluted in deionized water in a 96-well plate; each well contained 100μL of the diluted dye solution. Alternative, the dye dilutions were applied as 5mm spots on a nitrocellulose membrane, and integrated fluorescence emission over the specified wavelength range was measured using FONIRS. In addition, the membranes were scanned with Li-COR Odyssey, and the integrated density of signal in the 800nm channel, 16-bit, was measured using ImageJ software.

Preparation of fluorescent dextran, liposomes, and antibody

Dextran was labeled with IRDye 800 as follows. PBS solution of 500kDa amino dextran (10 mg/mL) was mixed with excess of IRDye800 for 1 hour at room temperature, followed by 24hrs of mixing at 4°C. *t*-BuOH was used to precipitate the labeled dextran and to remove the unreacted dye. This precipitation was repeated several times to eliminate the residual non-bound dye. The labeled dextran was resuspended in PBS at 10 mg/mL. PEGylated and non-PEGylated liposomes were prepared with 0.154mL of 25mg/mL Egg PC, 0.065mL of 4 mM DSPE-PEG 2000 (PEG liposomes only), and 0.002mL of 12.3mM DiR solutions in chloroform by evaporation-rehydration-vortexing method. The dry lipid cake was resuspended in 50μL PBS and subjected to three "freeze-thaw" cycles. The solution was brought to 1 mL by adding PBS, and was extruded using an Avastin manual extruder through 200nm-Whatman Nucleopore Track-Etch Membranes, through at least 15 extrusion cycles. Dialysis was performed with a 1000kDa Float-A-Lyzer Dialysis Device (Thermo Fisher) into 1L of PBS 3 times. A Zetasizer Nano (Malvern, UK) was used to confirm the size of the liposomes. To prepare liposomes loaded with dextran IRDye 680, dextran 3kDa was labeled with the dye and purified as described above, and the liposomes were

reconstituted with 10mg/mL solution of dextran in PBS instead of PBS. The subsequent steps for liposome preparation were the same as above.

Cetuximab was labeled with IRDye800 as follows. One hundred microgram of cetuximab in 50μL PBS was mixed with 2.2 μl of 3.02mM IRDye800-NHS in DMSO and the reaction was maintained at 4°C for 24 hrs. 100kDa Amicon Ultra Centrifugal Filters were used to wash the antibody and remove unreacted dye. The labeling density was determined with Nanodrop 2000C (Thermo Scientific) by measuring absorbance at 280nm (IgG) and 778nm (IRDye800). The absorbance of the dye at 280nm was experimentally determined as 0.0265 × A_{778nm} and subtracted from the total absorption A280. The labeling density was found to be ~1 dye per antibody.

In vivo monitoring of skin fluorescence

The University of Colorado IACUC approved all animal experiments (protocol 103913(11)1D). BALB/c mice (6–8 weeks of age) were anesthetized with ketamine/xylazine (1mg/0.16mg per mouse) and the right flank was depilated using Nair Hair Removal Cream. Skin was washed with warm water to prevent irritation from leftover cream. Mice were injected 24h later through the tail vein with labeled dextran, liposomes, or antibody. Blood was collected via the retro-orbital sinus from each mouse prior to injection and at different times post-injection. Two microliter spots were applied in duplicate on a 0.22 μm nitrocellulose membrane and scanned at 800 nm with Li-COR Odyssey. The spot integrated density of a 16-bit image was measured with ImageJ and plotted as a function of time with Prism (GraphPad, San Diego CA). A non-linear regression curve-fitting algorithm was used to fit the elimination profile into a mono- or bi-exponential decay to determine half-life. Skin fluorescence (integrated fluorescence) was measured with FONIRS as described in 3A in the depilated flank of each injected and non-injected mouse at the same time points as the blood drawing. Three skin scans per time point were taken, and each scan was the average of 2 scans with 800ms integration time. The signal values at 1 minute post-injection were set as 100% of injected fluorescence, and the data were normalized to this value. At different times post-injection, injected and non-injected (control) mice were sacrificed and the organs were isolated into a 12-well plate. Skin around the torso of each mouse was also collected after the final time point. Organs were scanned with Li-COR Odyssey (intensity of 1.0 at both wavelengths (700nm and 800nm)). Mean fluorescence of the organs was determined from 16-bit images using ImageJ software by subtracting the background, drawing a ROI around the organs, and using a measure function to determine mean gray value intensity per organ.

Skin digestion and quantification of fluorescence

To digest the skin, collagenase IV was prepared at 5mg/mL in 0.1% Tween-20 solution in PBS. Pieces of skin (4 per mouse) were weighed, minced, and placed into Eppendorf tubes. Tissue was mixed with 1:5 weight: volume equivalence of collagenase solution (e.g., 10mg tissue and 50μL digestion solution). Tissue was placed at 37°C and allowed to shake in a Thermomixer (Eppendorf) for 24 hours until completely digested. To generate a calibration curve, a liposomal solution was serially diluted with twofold dilutions from 1:20 to 1:320 using normal (non-injected) skin lysate as the dilution medium. Two microliters of each dilution and of the digested tissues were blotted on a nitrocellulose membrane with two dots

per dilution. The fluorescence was scanned using the Li-COR Odyssey. The images (16-bit) were used to measure integrated density per dot using ImageJ, and the amount of liposomes (nanoliter) per dot was calculated based on the calibration curve. This value was used to calculate % of injected dose per gram skin.

Statistical Analysis

The statistical analysis was performed using Prism 6 software. The differences between experimental groups were analyzed using a two-tailed parametric t-test assuming 95% confidence interval. Differences in all data are shown as *p<0.05; ***p<0.001; ****p<0.0001.

RESULTS

1) Fiber-optic-based near-infrared spectroscopy (FONIRS)

A FONIRS setup was constructed from commercially available and custom-made components as described in Fig. 1A–B and in Methods. The 760 nm LEDs delivered power output of 3.24 mW at the fiber end. The LEDs and filter setup were designed to match the excitation and emission wavelengths of commercially available NIR fluorophores (Table 1). The emission spectra were acquired using a Maya 200 Pro high-speed spectrometer, and the integrated fluorescence IF (area under curve) over the range of wavelengths was calculated (see Methods). As shown in Fig. 1C, FONIRS achieved low nanomolar sensitivity of detection of IRDye 800 dilutions in a microwell plate (~10 nM).

In order to determine sensitivity and linearity of detection of NIR fluorescence in the presence of skin, we prepared dilutions of a NIR dye DiR, spotted ~5mm diameter spots on a nitrocellulose membrane (Fig. 2A) and placed mouse skin (epidermis plus dermis, thickness ~0.25 mm) over each spot. To compare sensitivity, we used Li-COR Odyssey (Li-COR Biosciences) near-infrared scanner equipped with 700nm and 800nm solid-state lasers. According to Li-COR scans at 800nm (Fig. 2A), the fluorescence signal was readily detectable through the skin. Both Li-COR (Fig. 2B) and FONIRS (Fig. 2C) measurements show that the signal was linear within the range of 34–275 fmol DiR per spot. Based on these experiments and separate measurements of the normal skin background and noise (not shown), the sensitivity of FONIRS (skin background plus 3 standard deviations of the noise) was determined at 40 fmol DiR. In order to determine the penetration efficiency of FONIRS, we detected 135 fmol spot of DiR through multiple layers of mouse skin. According to Fig. 2D, there was an exponential attenuation of the IF, with an 85% drop in the signal at 4 skin layers. The lateral resolution of the fiber optics (at 1 mm distance between the probe tip and the sample) was experimentally determined to be ~4mm.

2) Longitudinal monitoring of accumulation of drug carriers in the skin

In a pilot *in vivo* experiment, we used IRDye 800-labeled dextran (500kDa) to determine the ability of FONIRS to detect fluorescence in the skin. We positioned the probe against the depilated flank of an anesthetized BALB/c mouse (Fig. 3A) and measured integrated fluorescence before, during and after systemic injection of dextran. The measurements were performed every 1.6 sec (minimal temporal resolution at the integration times used) for 25

min in order to detect fast kinetics of skin fluorescence post-injection. As shown in Fig. 3B, the fluorescence in the skin spiked during the injection phase, peaked at ~300 sec post-injection, and decreased by 13% at 2,200 sec post-injection. At the same time, levels of dextran in blood started to decrease immediately after the injection with a fast phase elimination half-life of 22 min (Fig. 3C and Supplemental Fig. 1), and 46% decrease at 2,200 sec post-injection. These experiments suggest that FONIRS measurements at initial time points likely reflect fluorescence of both circulating and skin-deposited fluorescence. Li-COR scans of skin pieces at 24 h (when dextran completely cleared from blood) showed significant accumulation of dextran (Fig. 3D).

In the second set of *in vivo* experiments, we performed a long-term monitoring of skin fluorescence after injection of a clinically approved anti-EGFR antibody cetuximab (ERBITUX™). Cetuximab was labeled with approximately one IRDye 800 per antibody (see Methods). Size of cetuximab is around 100Å, whereas the label size is ~20Å, suggesting that the antibody size should not significantly affected by labeling. The probe was positioned against a skin fold (Fig. 4A) in order to measure signal from the skin but not from the underlying tissues. Three measurements of integrated fluorescence were made at each time point to account for variability in the probe position and location relative to the skin Longitudinal monitoring with FONIRS showed a fast skin accumulation profile, peaking at 1h to 380% of the baseline skin level, and decreasing to 143% at 50h and 121% at 124h (Fig. 4B). At the same tine blood clearance profile showed half-life of 7h and complete elimination at 50h (Fig. 4C). Consistent with the FONIRS measurements, Li-COR scans of whole skin collected after the complete clearance of fluorescence from blood (124h) showed a significant antibody accumulation (Fig. 4D). In addition to the skin, the antibody accumulated in the liver, spleen and kidney, but not in the eyes, intestines, ovaries, pancreas, heart, lungs or muscle (Fig. 4E).

In the last set of *in vivo* experiments, we performed long-term monitoring of skin accumulation of liposomes. We prepared phosphatidylcholine (PC) liposomes labeled with DiR, with or without DSPE-PEG2000. Both formulations of liposomes (hereafter non-PEGylated and PEGylated) had similar size distribution (Table 2). Mice were injected intravenously with the same amount of fluorescence (corresponding to 0.55 nmol DiR). Skin fluorescence measurements showed that the signal from non-PEGylated liposomes jumped to 5000% of the baseline at 1 min post-injection but rapidly decreased to ~500% of the baseline (Fig. 5A and 5A insert). At the same time, PEGylated liposome fluorescence peaked more slowly (5000% of the baseline at 3h), and decreased to 900% of the initial level at 170h (Fig. 5A and 5A insert). Both types of liposomes were cleared from blood with a mono-exponential decay profile (Fig. 5B). PEGylated liposomes circulated much longer than non-PEGylated liposomes ($\tau_{1/2}$ 22h versus 1h). At 120h and 150h post-injection (when both types of liposomes were cleared from blood), PEGylated liposomes showed significantly higher signal in the skin than non-PEGylated liposomes.

Organ images (Fig. 5C) show that non-PEGylated liposomes accumulated in the skin, liver, spleen and small intestine, whereas PEGylated liposomes showed major accumulated in the eyes, liver, spleen, skin, small intestine, pancreas, kidneys and ovaries, with some deposition in muscle, heart, and lungs. Quantification of fluorescence showed that small intestine and

skin accumulated significantly more PEGylated liposomes than non-PEGylated liposomes (Fig. 5D). For both types of carriers, dermis contained significantly more fluorescence than epidermis (Supplemental Fig. 2). Control (non-injected) mouse did not show any fluorescence in these organs (Fig. 5D and Supplemental Fig. 3).

The accumulation of PEGylated liposomes in the skin is consistent with the clinical toxicity profile of Doxil [4]. In order to exclude the possibility that DiR dissociates from liposomes and transfers to cells, we collected blood from PEGylated liposome-injected mice and measured fluorescence of plasma and blood cells. According to Supplemental Fig. 4, over 97% of fluorescence was in plasma fraction, suggesting negligible transfer of the dye to the cell fraction. Furthermore, we tested whether fluorescence in the skin was associated with intact liposomes. PEGylated liposomes were internally loaded with 3kDa dextran-IRDye 680nm (Fig. 6A). Mice were injected with liposomes and sacrificed 200h later. Both DiR and dextran-IRDye 680 showed long circulation half-life in plasma, albeit dextran had a shorter half-life, suggesting partial leakage from liposomes in the circulation (Fig. 6B). However, both dyes showed co-localization in the skin and intestine (Fig. 6C–D), suggesting that some liposomes accumulate in the tissue together with the payload.

3) Estimation of skin deposition dose using FONIRS data

Lastly, we used FONIRS measurements to estimate the absolute dose of liposomes in the measured areas. We injected DiR labeled PEGylated liposomes into 4 nude mice, measured skin profile with FONIRS (Supplemental Fig. 5A), and harvested the skin at 200h post-injection (Supplemental Fig. 5B). Using a quantitative assay (see Methods) we determined the percentage of injected dose of PEGylated liposomes per gram of skin (% ID/g) using skin samples adjacent to the measured spot. As seen in Figure 7, skin contained on average 5.4±1.8% ID/g of liposomes. This value is similar to the calculated value of ~4% ID/g for Doxil at 170 hours post-injection [4]. Next, we estimated the % ID/g based on FONIRS measurements as follows. The integrated fluorescence *IF* measured longitudinally with FONIRS should be proportional to the concentration of the fluorophore in the skin (not distinguishing between intravascular blood pool and skin deposition. Since concentration in the tissue is in fact % ID/g, it is reasonable to assume that

$$\frac{\mathrm{IF}_t}{\mathrm{IF}_0}=\frac{\%\mathrm{ID}/g_t}{\%\mathrm{ID}/g_0} \quad (1)$$

where *IF* and %ID/g are the integrated fluorescence and tissue concentrations at time point 0 immediately after injection and at time t, respectively. Assuming % ID/g at the initial time point (1 min) is the concentration in blood multiplied by blood volume fraction in the skin (BVF, 8%), the initial concentration in the mouse skin should be:

$$\%\mathrm{ID}/g_0=\frac{100\%}{\mathrm{Weight}_{\mathrm{blood}}}\times \mathrm{BVF}=\frac{100}{1.7g}\times 0.08\%=4.7\% \quad (2)$$

According to equation (1), the concentration in the skin at a time point *t* for FONIRS measurement should be:

$$\%\mathrm{ID}/g_t = \frac{\mathrm{IF}_{12000\ \mathrm{min}}}{\mathrm{IF}_{1\ \mathrm{min}}} \times 4.7\% \quad (3)$$

Using the $\frac{IF_{12000\mathrm{min}}}{IF_{1\mathrm{min}}}$ value of each of the PEG liposome injected mice (Supplemental Fig. 5A), the estimated %ID/g skin value is 4.0±1.6% (Fig. 7), which is fairly close to the quantitative measurement (5.4% ID/g).

DISCUSSION

The main goal of the work was to develop and test a non-invasive and low-cost setup for longitudinal monitoring of deposition of drug delivery systems in the skin. Using FONIRS, we demonstrated significant skin deposition of dextran, antibody, and liposomes. Interestingly, PEGylated liposomes showed significantly higher deposition than non-PEGylated liposomes. This difference cannot be explained by the difference in the amount of injected fluorescence, since we injected the same amounts of non-PEGylated and PEGylated liposomes. Rather, the differences could reflect the deposition efficiency in the skin, clearance half-lives of these liposomes, and washout rates. The comparison of skin deposition were possible at later time points after the carriers completely had cleared from the circulation. At earlier time points, there was a contribution of blood borne fluorescence to the measurements. At the same time, by comparing blood clearance profile and skin fluorescence profile over time (Figs. 3,4,6), it is obvious that all the carriers show rapid buildup in the skin. The extent of skin accumulation partially correlated with the circulation half-life of the drug carriers. At the same time, the deposition of fluorescence in the skin could confound whole body NIR imaging studies as these are often performed to demonstrate localization in internal organs (tumors), or to demonstrate longevity of particles in systemic circulation. Therefore, this phenomenon of skin deposition has to be taken into account when performing nanoparticles pharmacokinetics studies using NIR imaging.

While the factors affecting drug carrier biodistribution and organ clearance have been studied before [1, 17] the mechanisms affecting skin deposition have not received much attention. To this end, we demonstrated that liposomes mainly deposit in the dermis layer. One explanation could be the binding and uptake by endothelial cells in the dermal capillaries. For example, dermal endothelial cells express mannose receptor[18] that recognizes dextrans [19]. Previous literature suggests that nanoparticles and liposomes are efficiently recognized by neutrophils and monocytes [20, 21], which suggests the deposition in the skin *via* homing of leukocytes. Interestingly, systemically injected quantum dots accumulate in the dendritic cells in the skin and then are drained by lymph nodes [5]. The mechanisms of the off-site toxicity of PEGylated doxorubicin liposomes were previously ascribed to extravasation in highly vascularized and inflamed sites and entrapment by macrophages and dendritic cells [3, 5]. On the other hand, Rakesh Jain's lab demonstrated

accumulation of Doxil in the endothelium in blood venules in the skin [22]. The mechanism of the skin deposition requires further investigation.

Using FONIRS measurements, we estimated the dose of liposomes in the skin (%ID/g). It must be kept in mind that the estimated value was obtained assuming homogenous distribution all over the body, whereas the actual accumulation in the skin is heterogeneous. This may explain the discrepancy between the estimated value and the actual quantification value (Fig. 7). To improve the accuracy of the estimate, it may be necessary to perform FONIRS measurements in more areas in the skin in order to determine the average IF. Besides flank measurements, it would be interesting to measure signal in the ears and in the eyes. In view of the high speed of measurements, multiple measurements are feasible and can provide researchers with a map of “hot” areas for a more accurate picture of distribution. Thus, for Doxil liposomes, skin areas on palms, foot and armpits were shown to be more prone to hand-foot syndrome [23].

Fluorescence deposition in the skin, albeit important by itself, could be potentially useful to estimate exposure in internal organs. For instance, there are a severe dose-limiting gastrointestinal side effects induced by the FDA approved liposomal irinotecan (ONIVYDE™)[24]. We observed a significant deposition of PEGylated liposomes in the intestines. A previous report showed that intestine and skin accumulated a significant amount of silica nanoparticles [6], suggesting that both intestine and skin could be important sink organs for nanoparticle accumulation. Ability to estimate intestinal deposition by the skin measurements could open enormous opportunities in monitoring patients and predict internal organ toxicity in the clinical setting. With further optimization and validation, FONIRS can be developed into an extremely useful tool to understand mechanisms of skin accumulation of xenobiotic drugs, for simultaneous tracking of multiple components (payloads) of nanoparticles in the skin, and for correlative preclinical and clinical studies to understand the link between skin deposition and organ toxicity.

Supplementary Material

Refer to Web version on PubMed Central for supplementary material.

Acknowledgments

The study was supported by the funding to DS: University of Colorado faculty startup fund, NIH R01 CA194058, NIH R21 CA167524, and Small Equipment Grant Program from the Associate Dean Research of Skaggs School of Pharmacy and Pharmaceutical Sciences, University of Colorado. Academic English Solutions (http://academicenglishsolutions.com/AES/home.html) revised the final paper.

REFERENCES

1. Li SD, Huang L. Pharmacokinetics and biodistribution of nanoparticles. Mol Pharm. 2008; 5:496–504. [PubMed: 18611037]
2. Yildirimer L, Thanh NT, Loizidou M, Seifalian AM. Toxicology and clinical potential of nanoparticles. Nano Today. 2011; 6:585–607. [PubMed: 23293661]
3. Lotem M, Hubert A, Lyass O, Goldenhersh MA, Ingber A, Peretz T, Gabizon A. Skin toxic effects of polyethylene glycol-coated liposomal doxorubicin. Archives of dermatology. 2000; 136:1475–1480. [PubMed: 11115157]

4. Gabizon A, Goren D, Horowitz AT, Tzemach D, Lossos A, Siegal T. Long-circulating liposomes for drug delivery in cancer therapy: a review of biodistribution studies in tumor-bearing animals. Advanced Drug Delivery Reviews. 1997; 24:337–344.
5. Sykes EA, Dai Q, Tsoi KM, Hwang DM, Chan WCW. Nanoparticle exposure in animals can be visualized in the skin and analysed via skin biopsy. Nat Commun. 2014; 5
6. Kumar R, Roy I, Ohulchanskky TY, Vathy LA, Bergey EJ, Sajjad M, Prasad PN. In vivo biodistribution and clearance studies using multimodal organically modified silica nanoparticles. ACS Nano. 2010; 4:699–708. [PubMed: 20088598]
7. Segaert S, Van Cutsem E. Clinical signs, pathophysiology and management of skin toxicity during therapy with epidermal growth factor receptor inhibitors. Annals of oncology : official journal of the European Society for Medical Oncology / ESMO. 2005; 16:1425–1433.
8. Dereure O. Drug-induced skin pigmentation. Epidemiology, diagnosis and treatment. Am J Clin Dermatol. 2001; 2:253–262. [PubMed: 11705252]
9. Cai W, Shin DW, Chen K, Gheysens O, Cao Q, Wang SX, Gambhir SS, Chen X. Peptide-Labeled Near-Infrared Quantum Dots for Imaging Tumor Vasculature in Living Subjects. Nano Lett. 2006; 6:669–676. [PubMed: 16608262]
10. Zavaleta CL, Garai E, Liu JT, Sensarn S, Mandella MJ, Van de Sompel D, Friedland S, Van Dam J, Contag CH, Gambhir SS. A Raman-based endoscopic strategy for multiplexed molecular imaging. Proceedings of the National Academy of Sciences of the United States of America. 2013; 110:E2288–E2297. [PubMed: 23703909]
11. Kong K, Kendall C, Stone N, Notingher I. Raman spectroscopy for medical diagnostics--From in-vitro biofluid assays to in-vivo cancer detection. Adv Drug Deliv Rev. 2015; 89:121–134. [PubMed: 25809988]
12. Stolik S, Delgado JA, Perez A, Anasagasti L. Measurement of the penetration depths of red and near infrared light in human “ex vivo” tissues, Journal of photochemistry and photobiology. B. Biology. 2000; 57:90–93. [PubMed: 11154088]
13. van Dam GM, Themelis G, Crane LM, Harlaar NJ, Pleijhuis RG, Kelder W, Sarantopoulos A, de Jong JS, Arts HJ, van der Zee AG, Bart J, Low PS, Ntziachristos V. Intraoperative tumor-specific fluorescence imaging in ovarian cancer by folate receptor-alpha targeting: first in-human results. Nature medicine. 2011; 17:1315–1319.
14. van der Vorst JR, Schaafsma BE, Hutteman M, Verbeek FP, Liefers GJ, Hartgrink HH, Smit VT, Lowik CW, van de Velde CJ, Frangioni JV, Vahrmeijer AL. Near-infrared fluorescence-guided resection of colorectal liver metastases. Cancer. 2013; 119:3411–3418. [PubMed: 23794086]
15. Judy RP, Keating JJ, DeJesus EM, Jiang JX, Okusanya OT, Nie S, Holt DE, Arlauckas SP, Low PS, Delikatny EJ, Singhal S. Quantification of tumor fluorescence during intraoperative optical cancer imaging. Scientific reports. 2015; 5:16208. [PubMed: 26563091]
16. Mohs AM, Mancini MC, Singhal S, Provenzale JM, Leyland-Jones B, Wang MD, Nie S. Hand-held spectroscopic device for in vivo and intraoperative tumor detection: contrast enhancement, detection sensitivity, and tissue penetration. Analytical chemistry. 2010; 82:9058–9065. [PubMed: 20925393]
17. Alexis F, Pridgen E, Molnar LK, Farokhzad OC. Factors affecting the clearance and biodistribution of polymeric nanoparticles. Mol Pharm. 2008; 5:505–515. [PubMed: 18672949]
18. Groger M, Holnthoner W, Maurer D, Lechleitner S, Wolff K, Mayr BB, Lubitz W, Petzelbauer P. Dermal microvascular endothelial cells express the 180-kDa macrophage mannose receptor in situ and in vitro. J Immunol. 2000; 165:5428–5434. [PubMed: 11067894]
19. Kato M, Neil TK, Fearnley DB, McLellan AD, Vuckovic S, Hart DN. Expression of multilectin receptors and comparative FITC-dextran uptake by human dendritic cells. Int Immunol. 2000; 12:1511–1519. [PubMed: 11058570]
20. Wang Z, Li J, Cho J, Malik AB. Prevention of vascular inflammation by nanoparticle targeting of adherent neutrophils. Nat Nanotechnol. 2014; 9:204–210. [PubMed: 24561355]
21. Inturi S, Wang G, Chen F, Banda NK, Holers VM, Wu L, Moghimi SM, Simberg D. Modulatory Role of Surface Coating of Superparamagnetic Iron Oxide Nanoworms in Complement Opsonization and Leukocyte Uptake. ACS Nano. 2015; 9:10758–10768. [PubMed: 26488074]

22. Yuan F, Leunig M, Huang SK, Berk DA, Papahadjopoulos D, Jain RK. Microvascular permeability and interstitial penetration of sterically stabilized (stealth) liposomes in a human tumor xenograft. Cancer Res. 1994; 54:3352–3356. [PubMed: 8012948]

23. Lorusso D, Di Stefano A, Carone V, Fagotti A, Pisconti S, Scambia G. Pegylated liposomal doxorubicin-related palmar-plantar erythrodysesthesia ('hand-foot' syndrome). Annals of oncology : official journal of the European Society for Medical Oncology / ESMO. 2007; 18:1159–1164.

24. Ko AH, Tempero MA, Shan YS, Su WC, Lin YL, Dito E, Ong A, Wang YW, Yeh CG, Chen LT. A multinational phase 2 study of nanoliposomal irinotecan sucrosofate (PEP02, MM-398) for patients with gemcitabine-refractory metastatic pancreatic cancer. British journal of cancer. 2013; 109:920–925. [PubMed: 23880820]

25. Upton RN. A model of the first pass passage of drugs from i.v. injection site to the heart--parameter estimates for lignocaine in the sheep. Br J Anaesth. 1996; 77:764–772. [PubMed: 9014631]

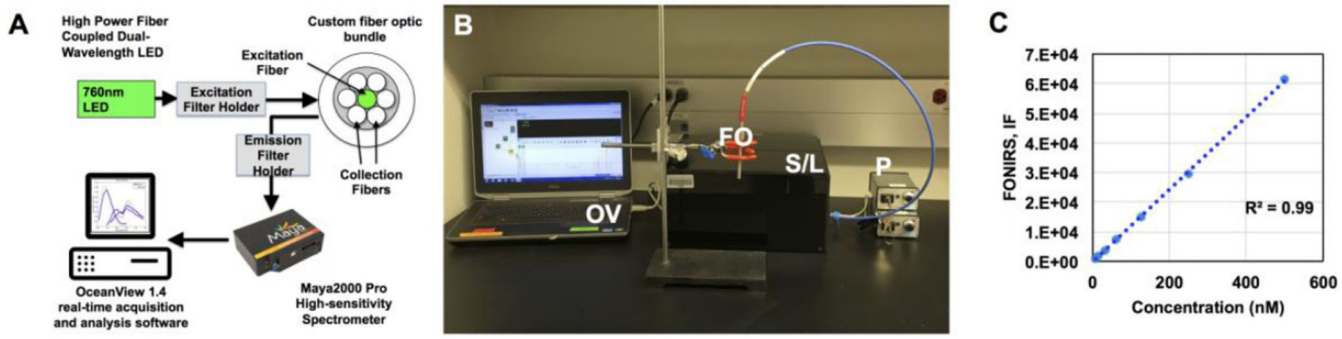

Fig. 1. FONIRS-Fiber-optic-based near-infrared spectroscopy system

A) System configuration; **B**) actual bench top setup. OV=OceanView software, FO=fiber-optic probe, S/L=spectrofluorimeter/LED in black enclosure, P=power source; **C**) Linearity and detection sensitivity of FONIRS using standard dilutions of IRDye800 in a 96-well plate. IF is the Integrated Fluorescence over the specified range of emission wavelengths (800–840nm).

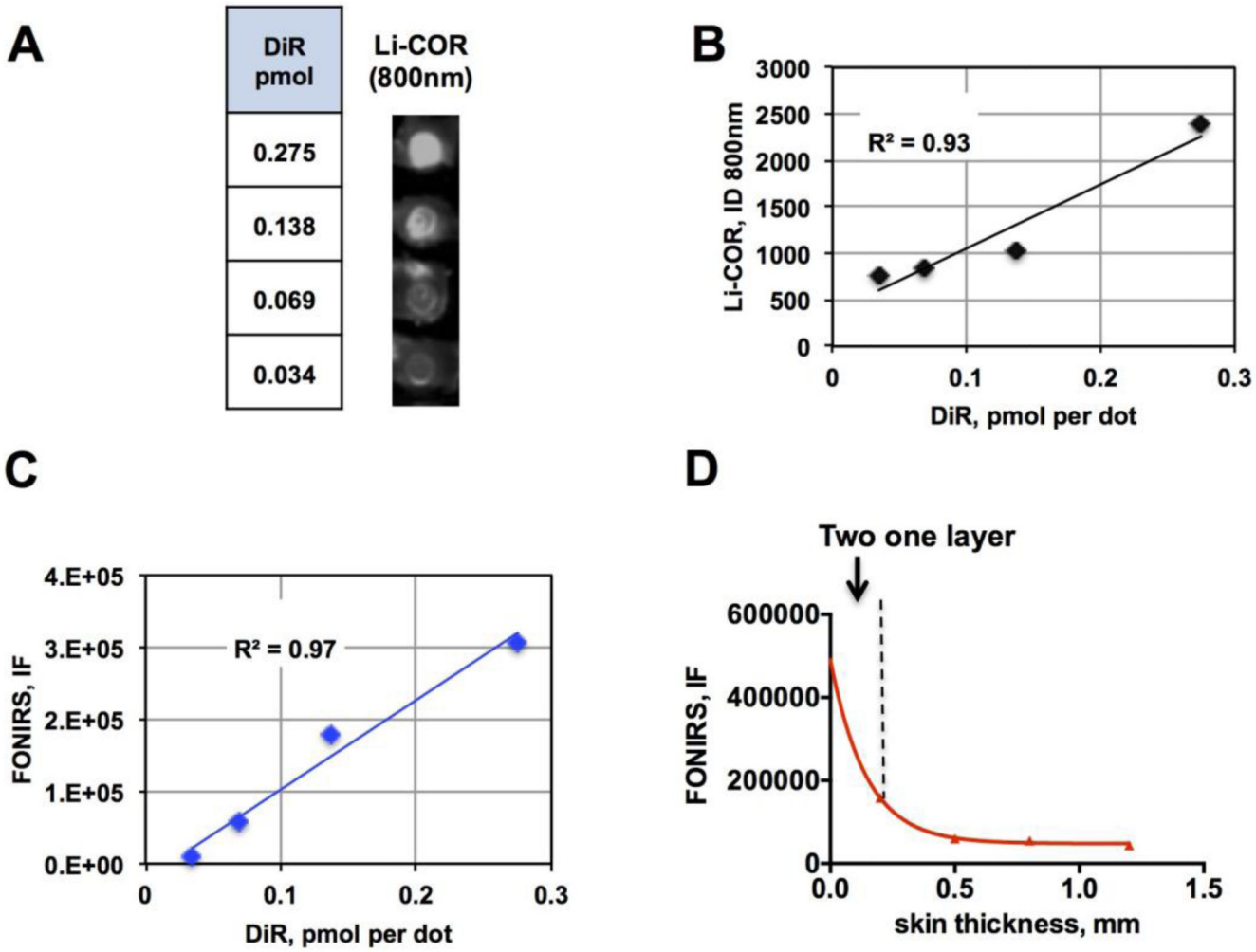

Fig. 2. FONIRS measurements of fluorescence ex vivo

A) DiR was spotted in different amounts on a nitrocellulose membrane (~5mm dots), and a square piece of depilated mouse skin (epidermis+dermis) was applied over each spot. The image shows a 800nm fluorescence scan (Li-COR) of different DiR amounts per spot with the skin layer on top; **B**) linear response of fluorescence in the presence of skin scanned with Li-COR. Integrated density of the spots was plotted against DiR amount per spot; **C**) Linear response of fluorescence in the presence of skin measured with FONIRS; **D**) Fluorescence of DiR measured with FONIRS over different numbers of mouse skin layers shows exponential decrease of the IF. The data were fitter with Prism software using monoexponential decay curve fit.

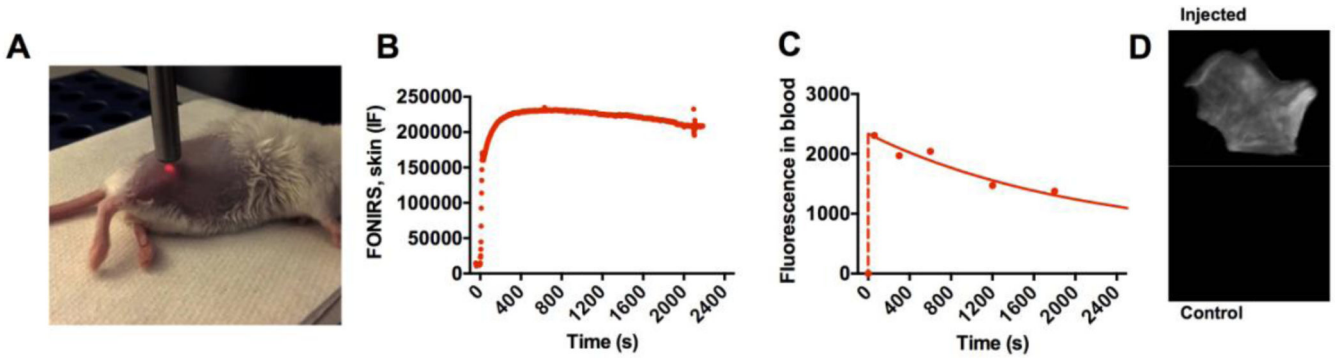

Fig. 3. Measurement of skin fluorescence with FONIRS in vivo

A) Anesthetized BALB/c mouse was depilated and positioned on its side. The image shows 760nm LED light on, with the probe almost touching the skin; **B**) mouse was injected with IRDye 800 labeled dextran (500kDa). Fast measurements of the integrated fluorescence over 2400 seconds show very low background signal before injection, immediate increase after the injection due to entrance of dextran into the blood pool, and relatively steady levels at 2400 s; **C**) blood fluorescence measurements show much fast elimination of dextran from blood. Data was fitted with Prism to bi-exponential decay. Full elimination profile and curve fit are shown in Supplemental Fig. 1; **D**) images of skin pieces scanned with Li-COR at 800nm (IRDye800) channel. Images of 24h post-injection show accumulation of dextran.

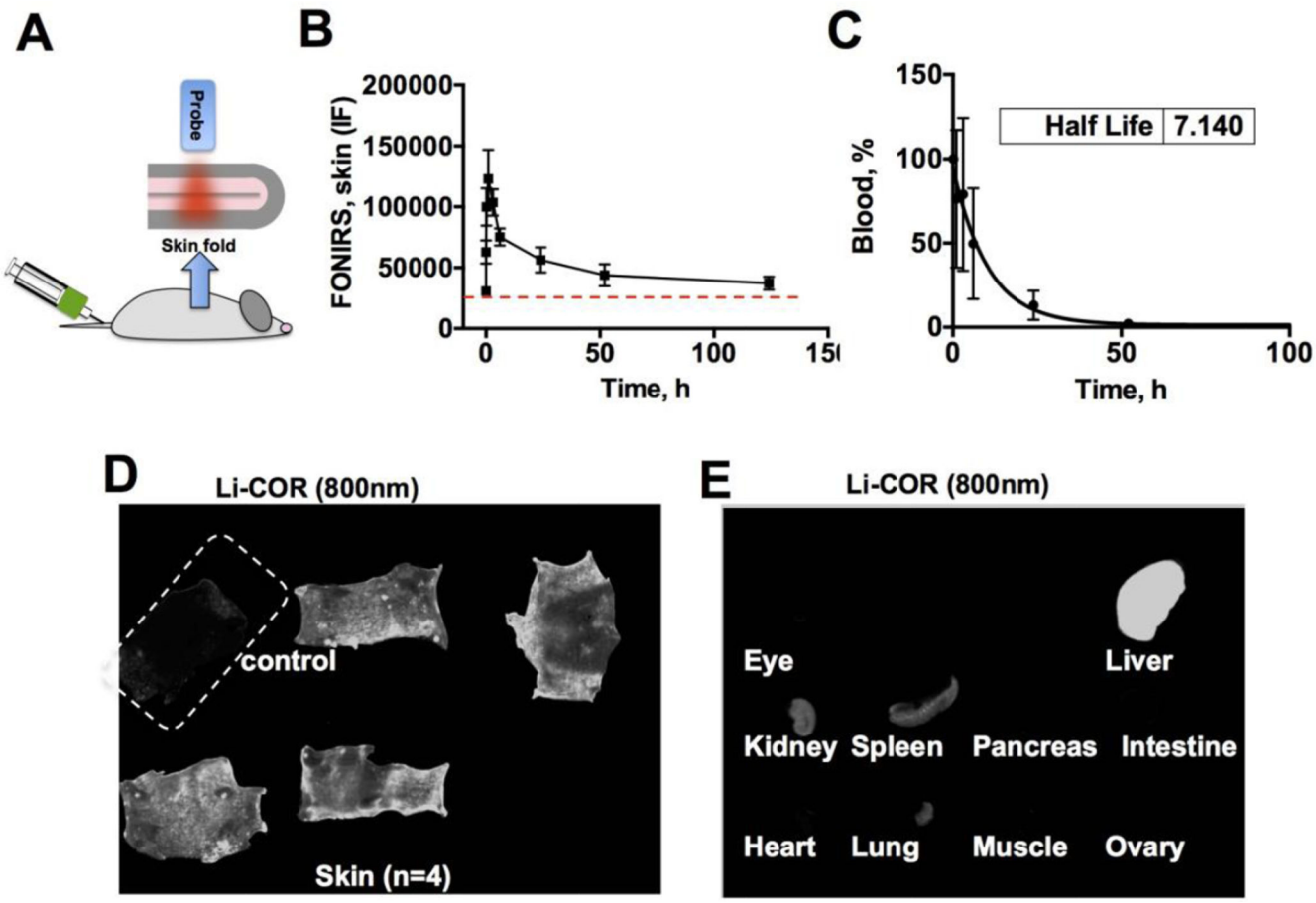

Fig. 4. FONIRS monitoring of mice injected with IRDye 800-labeled cetuximab

A) integrated fluorescence *in vivo* was monitored by forming a skin fold and positioning the probe against the skin. Fluorescence measurements were taken before the injection (baseline-dotted line) and as soon as 1 min post injection (the injected bolus mixes with blood at that time [25]) and continued for 124 hours; **B**) IF values of skin fluorescence were plotted against time (n=4).; **C**) blood half-life of cetuximab; **D**) *Ex vivo* whole skin scan with Li-COR (800nm channel) after the completion of the experiment (4 injected mice+1 control) show accumulation of fluorescence; **E**) Representative scans of internal organs (Li-COR 800nm channel). The brightness and contrast of skin and organs were adjusted to the same extent to improve presentation clarity.

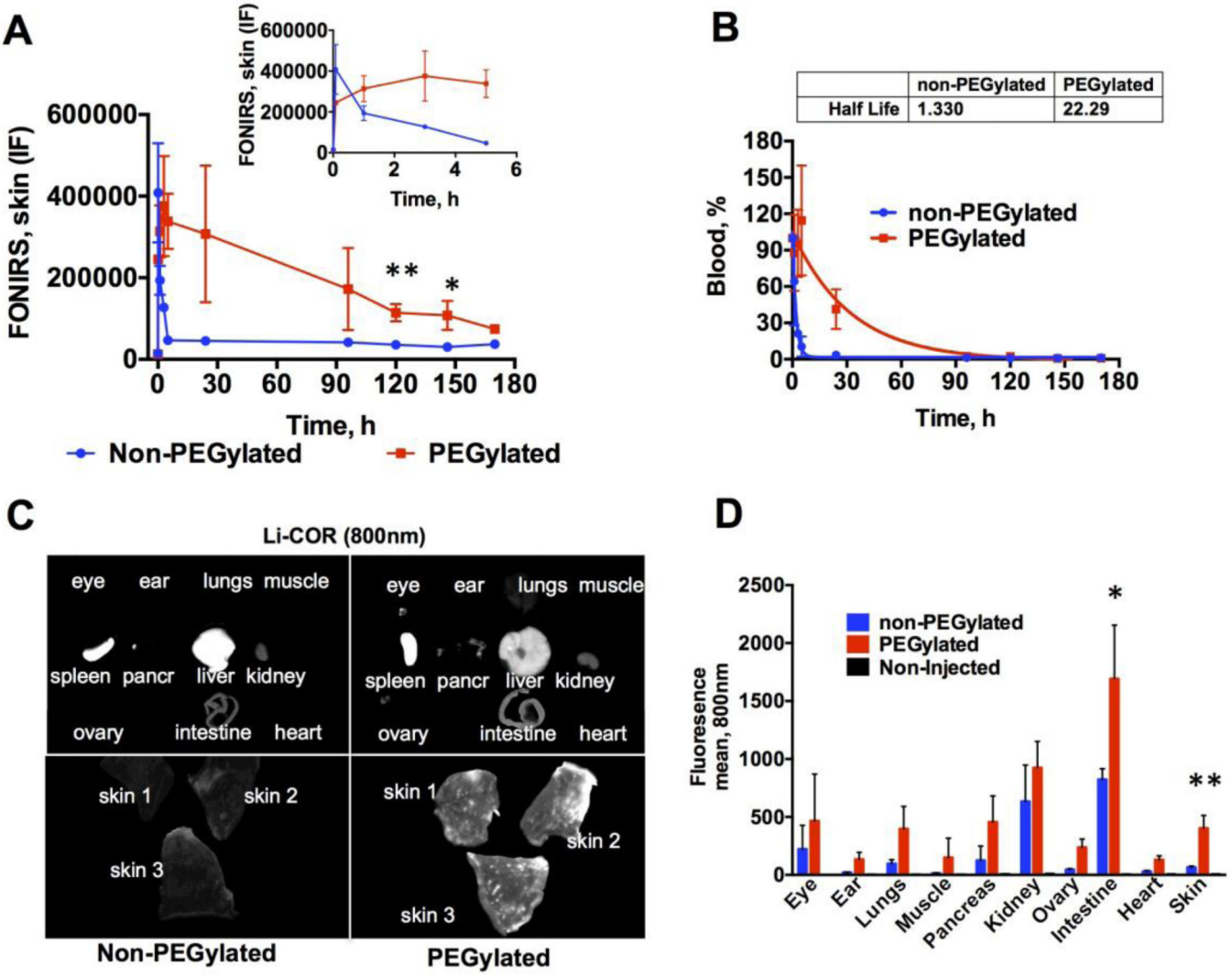

Fig. 5. FONIRS monitoring of mice injected with PEGylated or non-PEGylated liposomes (Table 2)

A) Mice were imaged as described in Fig. 4. DiR fluorescence spiked in the skin 1 min post-injection due to entrance of liposomes into the blood pool. Insert shows the initial time points after injection. At later time points, PEGylated liposomes showed significantly more accumulation compared to non-PEGylated liposomes (two-sided t-test, n=3). PEGylated liposomes showed slower buildup than non-PEGylated liposomes; **B**) circulation half-life was much longer for PEGylated liposomes than for non-PEGylated liposomes. Notably, fluorescence in the skin persisted beyond 100h (after the liposomes were cleared from blood); **C**) images of skin and organs scanned at 170h with Li-COR. Skin shows strong accumulation of PEGylated liposomes. Consistent with longer blood half-life, there was lower accumulation of PEGylated liposomes in the liver than non-PEGylated liposomes; **D**) quantification of mean fluorescence intensity (800nm) in the internal organs. PEGylated liposomes showed a significant accumulation in the skin, kidney, and small intestine. Liver and spleen were not included in the graph. Two-sided t-test; n=3, *p<0.05; **p<0.01. The

brightness and contrast of skin and organs were adjusted to the same extent to improve presentation clarity.

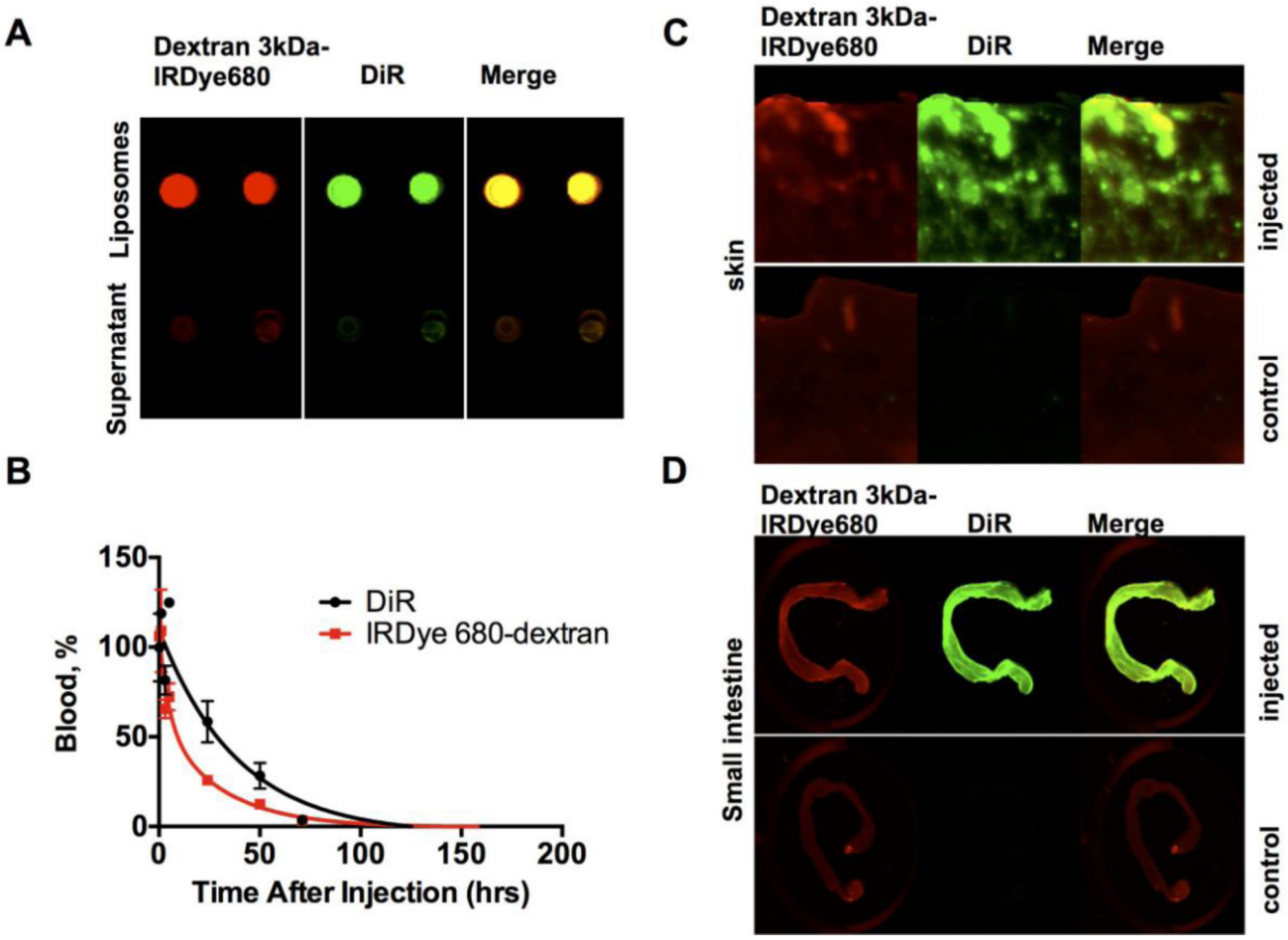

Fig. 6. Skin accumulation of DiR labeled liposomes loaded with 3kDa dextran-IRDye 680

A) Dual-labeled liposomes were washed by dialysis, pelleted with ultracentrifuge, spotted on a nitrocellulose membrane and imaged with Li-COR odyssey (800nm-DiR; 700nm-IRdye680). There was no free dye in the solution (supernatant) after centrifugation; **B**) circulation of liposomes in mice after systemic injection. Both DiR and dextran showed long half-life, albeit dextran had a shorter half-life, likely do to partial release from liposomes in vivo and faster clearance than liposomes (n=2); **C–D**) Accumulation of fluorescence in the skin and small intestine (scanned with Li-COR after sacrificing the mice 200 h post-injection). Colocalization of DiR and dextran-IRDye 680 in the skin and intestine suggests that liposomes arrive with the payload to the tissue. Control non-injected mice show some signal in the 700nm channel (autofluorescence).

	Actual	Predicted
Mean	5.371	3.953
Std. Deviation	1.839	1.606

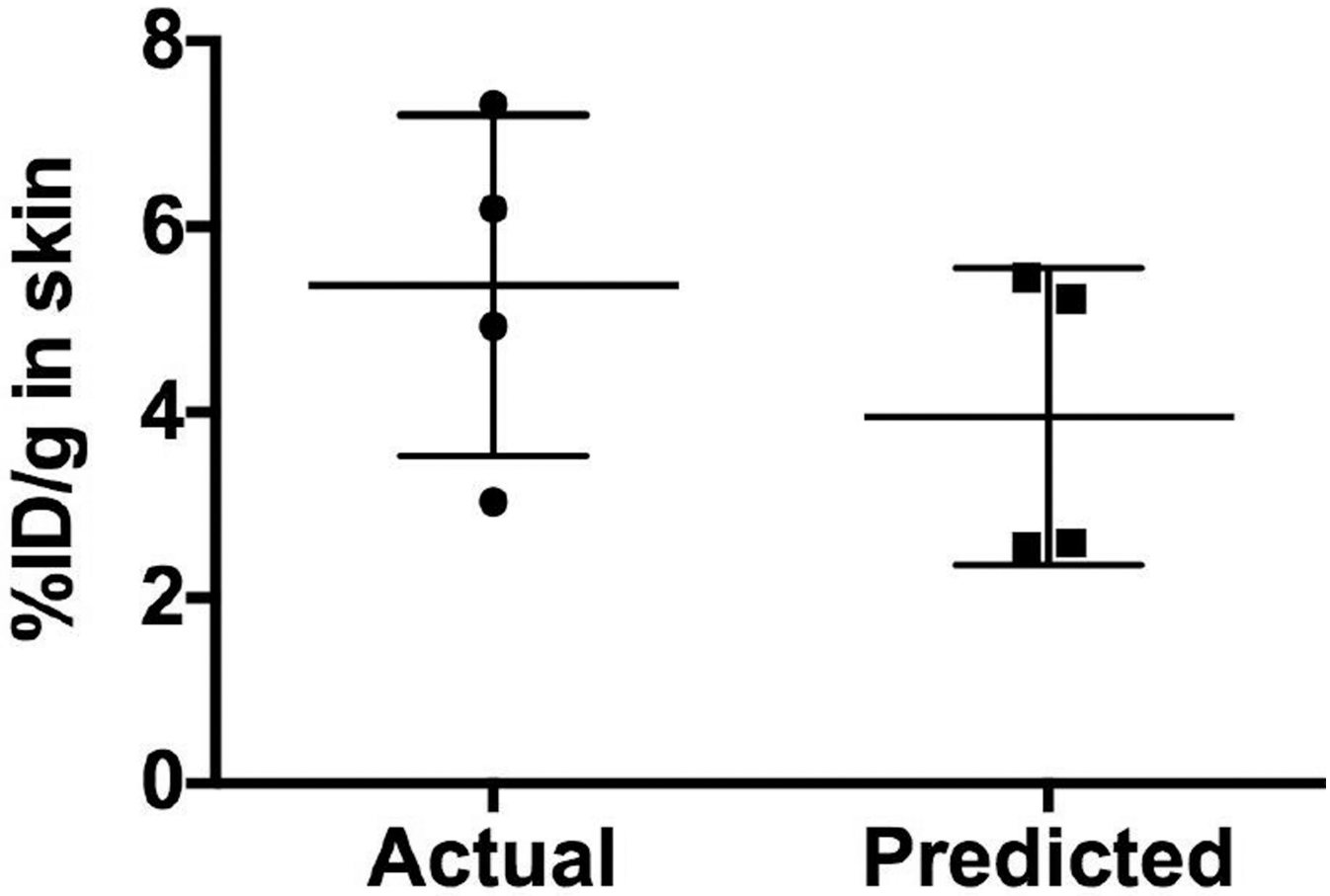

Fig. 7. Predicted versus actual percentage of injected dose per gram skin (%ID/g) for PEGylated liposomes

Deposition of liposomes was quantified as described in Methods using 4 skin samples per mouse (Supplemental Fig. 5). Individual points show average value for each mouse (n=4). The predicted values were calculated as described in the Results section using FONIRS data from 4 mice per group (Supplemental Fig. 5A). Predicted values agreed well with the actual values.

Table 1

Properties of fluorophores used in the study and the optical setup

Spectral channels (LED)	**760nm**		**670nm**
Filter settings	**Ex: 785nm short pass/Em: 785nm long pass**		**Ex: 692nm short pass/Em: 694nm long pass**
Fluorophore	DiR	IRDye800	IRDye680
Peak Excitation	750nm	778nm	680nm
Peak Emission	773nm	774nm	694nm
Extinction Coefficient (ε; $M^{-1}cm^{-1}$)	199,000	300,000	170,000

Table 2

Size of liposomes used in the study

Liposome formulation	Intensity weighted diameter	Polydispersity index
PC/DiR	135	0.23
PC/DSPE-PEG/DiR	174	0.128
PC/DSPE-PEG/DiR/dextran 3kDa-IRDye 680	145	0.129